

REPORT DOCUMENTATION PAGE			Form Approved OMB NO. 0704-0188	
Public reporting burden for this collection of information is estimated to average 1 hour per response, including the time for reviewing instructions, searching existing data sources, gathering and maintaining the data needed, and completing and reviewing the collection of information. Send comment regarding this burden estimate or any other aspect of this collection of information, including suggestions for reducing this burden, to Washington Headquarters Services, Directorate for Information Operations and Reports, 1215 Jefferson Davis Highway, Suite 1204, Arlington, VA 22202-4302, and to the Office of Management and Budget, Paperwork Reduction Project (0704-0188), Washington, DC 20503.				
1. AGENCY USE ONLY (Leave blank)		2. REPORT DATE		3. REPORT TYPE AND DATES COVERED REPRINT
4. TITLE AND SUBTITLE  TITLE ON REPRINT			5. FUNDING NUMBERS  ARO MIPR 96-20	
6. AUTHOR(S)  AUTHOR(S) ON REPRINT				
7. PERFORMING ORGANIZATION NAMES(S) AND ADDRESS(ES)  NORTHWESTERN UNIVERSITY DEPARTMENT OF PHYSICS AND ASTRONOMY EVANSTON, ILLINOIS 60208			8. PERFORMING ORGANIZATION REPORT NUMBER	
9. SPONSORING / MONITORING AGENCY NAME(S) AND ADDRESS(ES)  U.S. Army Research Office P.O. Box 12211 Research Triangle Park,, NC 27709-2211			10. SPONSORING / MONITORING AGENCY REPORT NUMBER  ARO 33104.2-MS	
11. SUPPLEMENTARY NOTES  The views, opinions and/or findings contained in this report are those of the author(s) and should not be construed as an official Department of the Army position, policy or decision, unless so designated by other documentation.				
12a. DISTRIBUTION / AVAILABILITY STATEMENT  Approved for public release; distribution unlimited.			12 b. DISTRIBUTION CODE	
13. ABSTRACT (Maximum 200 words)  <div style="display: flex; align-items: center;"> <div style="writing-mode: vertical-rl; transform: rotate(180deg); font-weight: bold; margin-right: 10px;">DWC QUALITY INSPECTED 4</div> <div>ABSTRACT ON REPRINT</div> </div>				
14. SUBJECT TERMS			15. NUMBER IF PAGES	
			16. PRICE CODE	
17. SECURITY CLASSIFICATION OF REPORT  UNCLASSIFIED	18. SECURITY CLASSIFICATION OF THIS PAGE  UNCLASSIFIED	19. SECURITY CLASSIFICATION OF ABSTRACT  UNCLASSIFIED	20. LIMITATION OF ABSTRACT  UL	

C. J. Kuehmann and G. B. Olson, "Computer-aided systems design of advanced steels," in: *International Symposium on Phase Transformations During the Thermal/Mechanical Processing of Steel - Honouring Professor Jack Kirkaldy*, E. B. Hawbolt, et al., eds., The Metallurgical Society of the Canadian Institute of Mining, Metallurgy and Petroleum, Vancouver, British Columbia (1995) 345-356.

### Computer-Aided Systems Design of Advanced Steels

Dr. Charles J. Kuehmann, BIRL Industrial Research Laboratory: Ferrium Division, 1801 Maple Avenue, Evanston, Illinois 60201-3135 USA

Professor Gregory B. Olson, Northwestern University, Department of Materials Science and Engineering, 2225 North Campus Drive, Evanston, Illinois 60208 USA

### ABSTRACT

The multi-institutional interdisciplinary research program of the Steel Research Group (SRG) has centered on the development of a systems approach for the design of advanced high-performance steels using computer-aided modelling. Initial long range studies involved the development of the theoretical foundations underlying strength, toughness, and hydrogen resistance. Mechanistic based computational models include the prediction of martensite start temperatures in high alloy steels, multicomponent coarsening kinetics in non-ideal non-dilute systems, and the martensitic transformation volume change in multicomponent systems. Modelling has successfully related the peak hardness in secondary hardening steels to the coherent driving force of the  $M_2C$  carbide in para-equilibrium with transient cementite. Additionally, the precipitation time scale has been related to the multicomponent coarsening coefficient of the  $M_2C$  carbide with respect to the half-completion state. Within a systems design framework, these models have been successfully applied to the design of high performance alloys including stainless bearing steels, advanced armor steels, and high-hardness gear steels.

19970514 165

## INTRODUCTION

As an innovator in the use of computational metallurgy, Prof. Jack Kirkaldy, was an early pioneer in the use of computer power applied to both the fundamental study and commercial development of steel. His work has inspired a generation of researchers to dedicate their careers to this field. Recently, the computational modelling of phase transformations occurring during thermal/mechanical processing of steels has become more complex yet less expensive as computational capabilities have increased and the cost of computing power has decreased. At the same time, experimental investigative techniques have also advanced, utilizing the latest developments in characterization methods, albeit at ever increasing cost. This new relative cost structure relating computational modelling and empiricism is driving a revolution in the way in which steels are developed. Historically, the development of steels followed a largely empirical path in which qualitative models drove empirical studies leading to the development of a new alloy. The new paradigm of alloy design reverses these traditional roles. Computational modelling can now perform the detailed simulations of the microstructural response to thermal/mechanical processing required to determine a new alloy composition while empiricism validates the computer models and determines the optimum processing of a new alloy. Thus empirical studies now drive the development of computational models leading to the design of a new steel. Ferrous metallurgy, containing a wealth of prior mechanistic and empirical knowledge, possesses a distinct advantage for the development of computational modelling and is at the forefront of this revolution.

Development of the computational models must reflect the manner in which they are to be used. In this work, the modelling is part of a general systems approach to the design of materials. The systems design of materials builds on the universal systems engineering approach described by G. M. Jenkins[1] and the concept of materials as systems by Cyril Smith[2] describing material structure as a hierarchy of interacting microstructural subsystems. This approach is further expanded to describe the hierarchial nature of processing and material properties[3] using a linear processing-structure-properties-performance model of materials science depicted by the three-link chain model of Figure 1. An example of this hierarchial description is given in the flow-block diagram of secondary hardening ultrahigh-strength steel of Figure 2. The flow block diagram illustrates the influence processing steps have on the microstructural components of the matrix, strengthening dispersion, austenite dispersion, grain refining particles and grain boundary chemistry and the resulting desired properties of strength, toughness and hydrogen resistance. Describing each of these components as a set of interacting subsystems arranged in a hierarchial manner, computational modelling serves the role of providing quantitative descriptions of the interactions between subsystems. In order to be successful, the modelling must be mechanistic and quantitative in nature. Mechanistic computational models can be used as predictive design tools, capable of extrapolation, while empirically based models are interpolative and limited to problems in which the solution is known to lie within the bounds of the model.

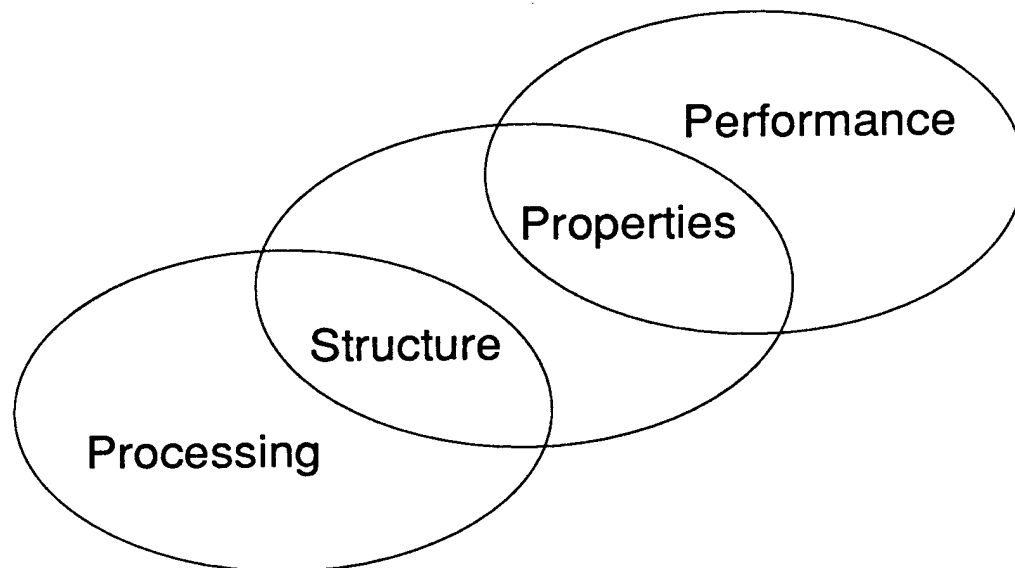


Figure 1 - Three-link chain model of materials science illustrating the linear processing-structure-properties-performance description.

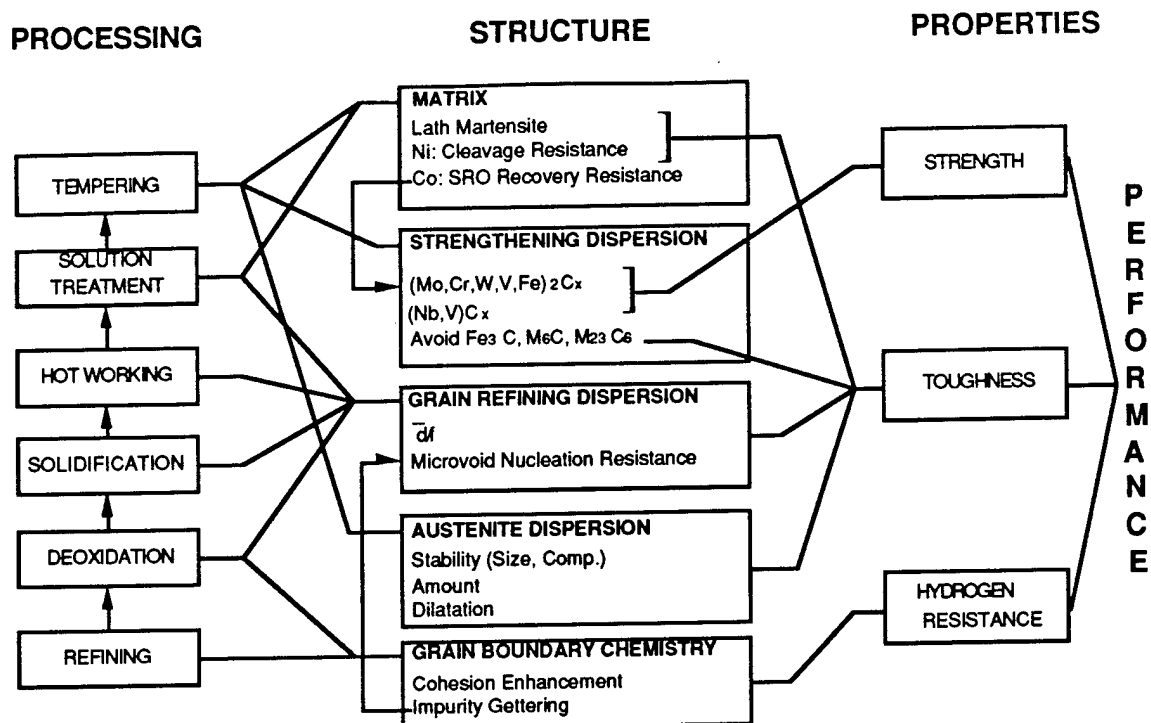


Figure 2 - Flow-block diagram for secondary hardening ultra-high strength steels.

The Steel Research Group (SRG), a multi-institutional research program comprised of members from industry, academia, and government, was initiated in 1985 to combine physical metallurgy, applied mechanics, physics, and chemistry in order to establish the basic principles underlying the processing-structure-properties relations in steels and apply this understanding to the design of superior alloys. The goal of this effort consists of the development of broad based quantitative relationships to describe the processing-structure and structure-property interplay and a systems approach to using these tools that lead to the creation of improved alloys. The development of quantitative models for the prediction of alloy behavior is well under way and the recent focus is centered on the framework in which to use these tools to improve alloys. As this framework is developed, new insights into the basis of the modeling tools are found and, subsequently, the models are improved. In this manner, a coherent approach to the understanding of given material systems is achieved that allows direct application to technologically important problems. Recently, the Ferrium Division of Northwestern University's BIRL Industrial Research Laboratory was established to pursue the application of these models and techniques to the development of proprietary alloys and processes for industry. This paper will review key computational modelling efforts of the SRG/Ferrium Division and provide an example of how they are used in alloy design using the systems approach.

## COMPUTATIONAL MODELS

A vital component of the modelling we have undertaken is the ThermoCalc thermochemical databank system(4) developed at the Royal Institute in Stockholm. The ThermoCalc program uses thermodynamic assessments from binary, ternary, and quaternary systems to extrapolate to higher order systems. Equilibria, constrained equilibria, and driving forces can be calculated as functions of composition, chemical potential, as well as user defined functions. Central to the versatility of the program is a separation of the calculation package from the database, simplifying the ability to use different thermochemical models to describe the thermodynamics of the system. The ThermoCalc software offers unprecedented access to equilibrium thermodynamic quantities for complex, high-order systems. To apply this information to the modelling of highly nonequilibrium processes of interest in real alloys, we describe the dynamic nature of phase transformations in terms of thermodynamic scaling factors which can then be evaluated by the software. The first computational model that we review is based on this approach and involves the precipitation of  $M_2C$  carbides leading to the secondary hardening response in ultrahigh-strength steels. The second modelling effort we shall review involves the application of first principles quantum mechanical calculations to the design of steels with improved resistance to hydrogen embrittlement and intergranular fracture.

## Secondary hardening

Ultrahigh-strength (UHS) secondary hardening steels are strengthened by the precipitation of coherent  $M_2C$  carbides during tempering. In high Co steels in which dislocation recovery is retarded, the  $M_2C$  carbides precipitate coherently on dislocations and provide the characteristic secondary hardening peak during tempering. The SRG conducted a deliberate and comprehensive investigation of this phenomenon in commercial and model alloys in order to gain a fundamental understanding of the process and develop a quantitative design model. A wide range of techniques were utilized to gather experimental information across the complete range of size and time scales of interest. Atom-probe field-ion microscopy (APFIM)[5,6], transmission electron microscopy (TEM)[7], small angle neutron scattering (SANS)[8], and X-ray diffraction (XRD)[7,9] techniques provided information on the size, shape, composition, and lattice parameters of the  $M_2C$  precipitates as well as the resulting hardness values spanning tempering times of less than an hour to more than a thousand hours. This study identified that the precipitation was well described by the theory developed by Langer and Schwartz[10] for precipitation at high supersaturation in which the growth regime is suppressed and precipitation occurs by a process of nucleation and coarsening, maintaining a particle size close to the critical size.

Based on these investigations, two important scaling factors are identified. The initial critical nucleus determines the size scale of the precipitates throughout the precipitation reaction and the coarsening rate constant determines the precipitation time scale. Both of these factors are vital to the successful design of a UHS steel. The peak hardness in a UHS steel commonly occurs at the particle size corresponding to the transition from particle shearing to Orowan bypass. It is also advantageous to bring the  $M_2C$  precipitation to completion in order to dissolve all of the transient cementite which otherwise limits toughness. Therefore, the smaller the initial critical particle size, the closer completion of precipitation occurs to peak hardness and more efficient strengthening is obtained. The time scale of precipitation is also important due to the kinetic competition between the secondary hardening reaction and the segregation of impurities to the prior austenite grain boundaries leading to intergranular embrittlement.

The initial critical nucleus size scales inversely with the thermodynamic driving force for precipitation. In the case of the  $M_2C$  carbide it is important to include the influence of prior cementite formation and coherency on this quantity. The coherency elastic self energy can be evaluated by the calculation of an anisotropic ellipsoidal inclusion using the equivalent eigenstrain method[11] and the impact of solute redistribution on the resulting stress distribution is addressed by using open-systems elastic constants[12]. By relating the coherency strain to composition via the compositional dependence of the particle and matrix lattice parameters, the compositional dependence of the elastic self energy is determined in a form compatible with the ThermoCalc software. The linear elastic self energy calculation represents an upper limit and a correction factor is used to fit the precipitation composition trajectories of a large set of experimental alloys. The impact of prior cementite precipitation is accounted for by the calculation of the coherent driving force in the presence of the carbon potential due to para-equilibrium cementite. This para-equilibrium carbon potential is defined by an equilibrium between the matrix and cementite in which the substitutional species are held constant and only the interstitial carbon is allowed to partition. In this approximation the cementite acts as a carbon source at constant chemical potential.

Figure 3 represents the level of agreement of the strengthening response of the model alloys with the above model. The model alloys contain 16 wt% Co, 5 wt% Ni, and 0.24 wt% C with varying amounts of the carbide formers Cr, Mo, and, in a few cases, V. The nickel content is chosen to eliminate austenite precipitation during tempering which otherwise complicates the hardening response. In Figure 3, the peak hardness during tempering at 510 C is plotted against the driving force for precipitation of the coherent  $M_2C$  carbide in the presence of para-equilibrium cementite. The open circles represent alloys containing V. The relationship demonstrates the ability to predict peak hardness values within approximately  $\pm 25$  VHN in this class of alloys. Work continues to correlate driving force directly to critical particle size and interparticle spacings.

The time scale of precipitation at high supersaturations, according to the Langer-Schwartz treatment, scales with the coarsening rate of the particle distribution. The modelling pursued in this work expands upon the Lifshitz-Slyozov and Wagner (LSW)[13,14] theory, describing the coarsening of spherical particles in a binary system, with the intent of removing the binary restrictions of the LSW theory and reformulating it in a manner compatible with the multicomponent thermodynamics of the ThermoCalc software. Initially, this work involved the extension of the LSW treatment to ternary systems[15] and was later expanded to the more general multicomponent case[16]. The result of this analysis characterizes the coarsening rate of a particle of average size as a function of the multicomponent diffusion coefficients, the equilibrium partitioning coefficients, and the second derivatives of the Gibbs free-energy evaluated at the equilibrium state. The surface energy and molar volume are taken to be composition independent and are considered constant. In this form, the coarsening rate constant is the result of an asymptotic analysis and is only representative at very long time scales and very close to equilibrium. This is certainly not the case for the precipitation of the  $M_2C$  carbide at high supersaturation. The matrix content of alloy is far from equilibrium during much of the precipitation process, approaching equilibrium only near completion. This effect is most severe for alloys containing stoichiometric quantities of carbide

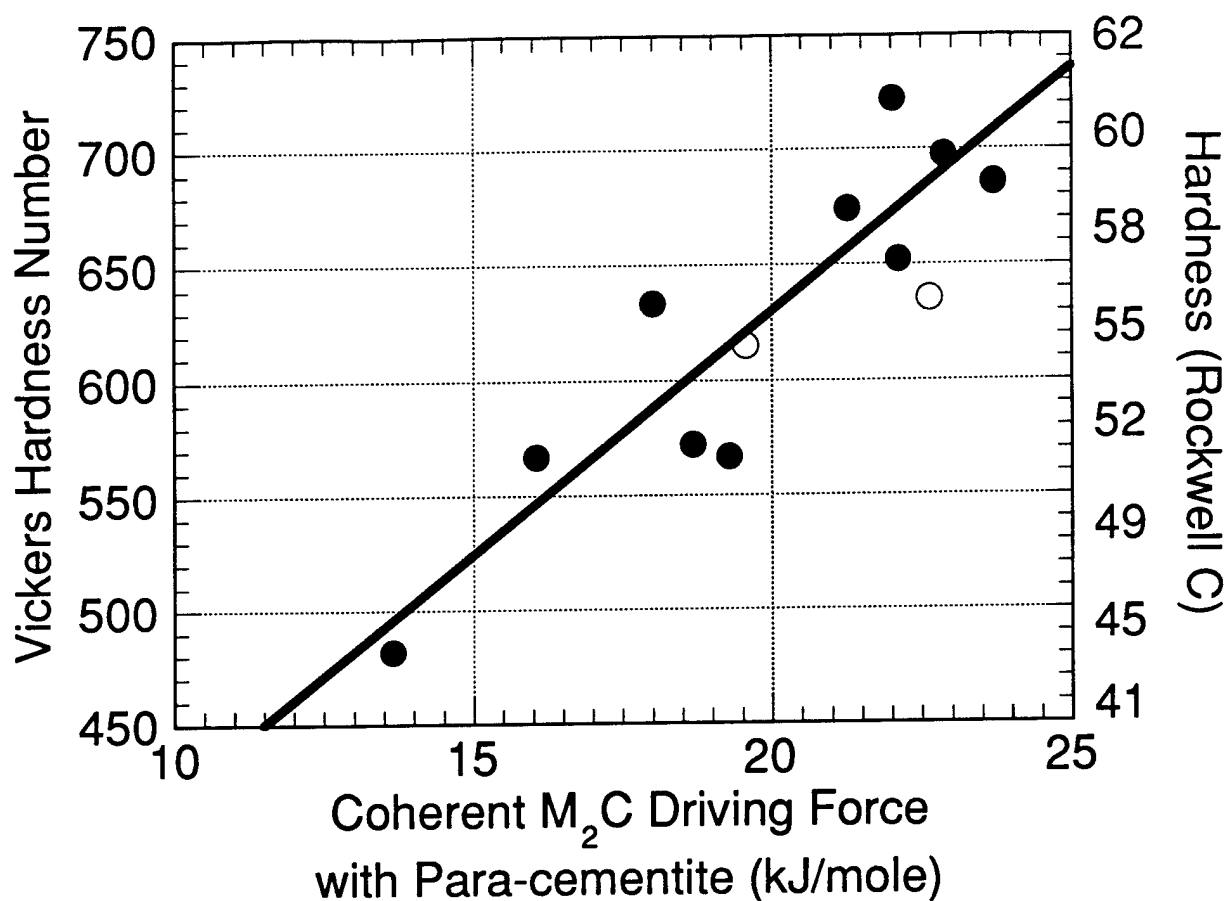


Figure 3 - Correlation of peak hardness during tempering at 510 C to the coherent driving force for the precipitation of  $M_2C$  carbide in the presence of paraequilibrium cementite.

formers as measured by the relative difference in the matrix alloy content during precipitation and at equilibrium. During precipitation in a stoichiometric alloy, the alloy matrix content is of the same order as the overall alloy content, while at equilibrium, the matrix alloy content is very small. To define a coarsening rate constant more representative of the conditions present during the precipitation process, a coarsening rate is evaluated at the point when the volume fraction of the precipitate is one-half of the equilibrium value. This is achieved by calculating the coherent equilibrium for the  $M_2C$  carbide, and then, adding energy to the  $M_2C$  phase to account for capillarity until the amount of the phase is half of the equilibrium value. The coarsening rate is then calculated from the thermodynamic properties of this state. Figure 4 represents the correlation between the precipitation half-completion time and the half-completion coarsening rate constant of the model alloys for which this data is available. The experimental data spans a kinetic range of over two decades and the correlation holds to within a quarter decade over the range.

### Interfacial Cohesion

Hydrogen embrittlement of ultrahigh-strength steels is associated with the prior segregation to the grain boundary of impurities such as P and S. A thermodynamic treatment of this phenomenon by Rice and Wang[17,18] illustrates that the potency of a segregating solute in reducing the work required for brittle fracture along a boundary is linearly related to the difference in the segregation energy for the solute at the boundary and at the free surface. Specifically, a solute with a higher segregation energy at the free surface will be an embrittler while a solute with a higher segregation energy at the grain boundary will enhance intergranular cohesion. A survey of reported segregation energies and embrittling potency (reported as the shift in the ductile-to-brittle transition temperature per atomic percent solute on the grain boundary) in Fe-base alloys demonstrates these general trends[17]; however, the experimental difficulty of surface thermodynamic measurements gives ambiguous values for some solutes.

A study was undertaken by the Steel Research Group at Northwestern University to use state-of-the-art total-energy electronic-structure calculations and advanced supercomputer processing to investigate the

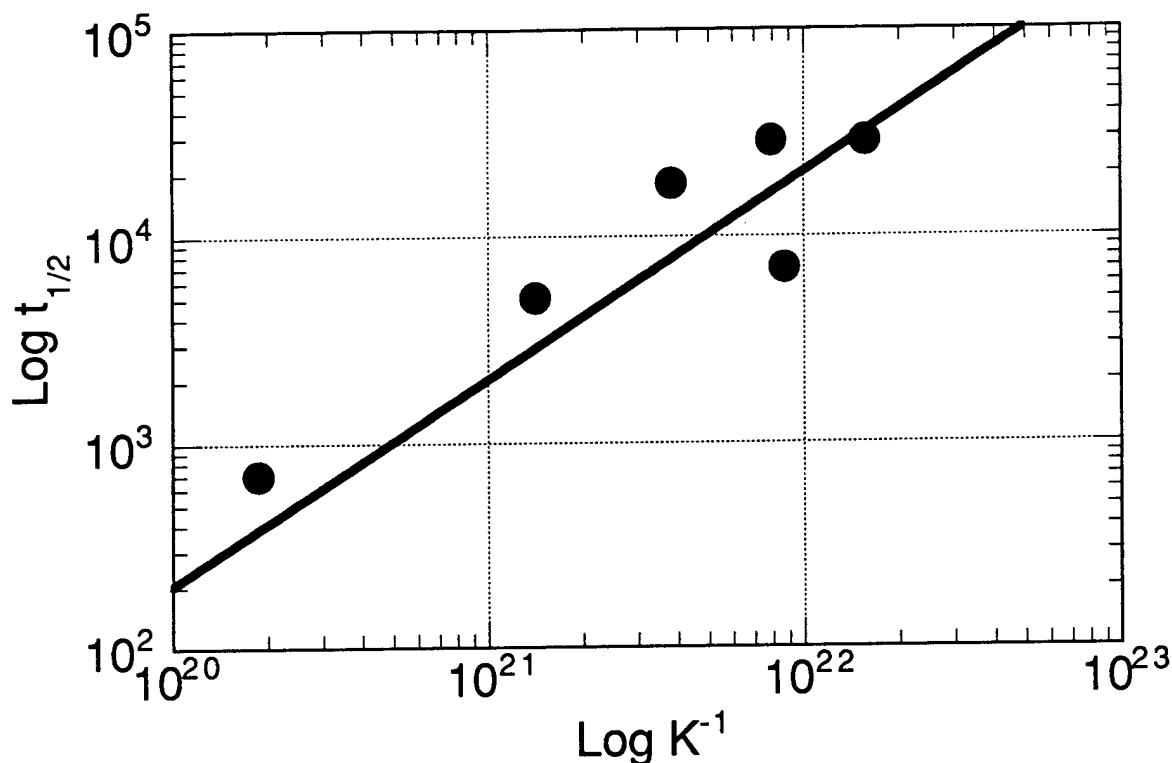


Figure 4 - Correlation of the half-completion time with the half-completion coarsening rate constant for a number of model alloys tempered at 510 C.

electronic basis of intergranular embrittlement in light of the Rice-Wang theory[19]. In the study, first principles calculations were used to determine the total energy of atomic cells representing the Fe  $\Sigma 3[110](111)$  grain boundary and (111) free surface with a monolayer of an impurity solute present. The calculations were accomplished with the full-potential linearized plane wave (FLAPW) total energy technique. The atomic structure in each case was relaxed to find the minimum energy state. The results of these calculations include not only the segregation energies responsible for the embrittling or cohesion enhancing effects of segregating solutes, but the underlying electronic structure of the solutes in the boundary and surface environments. A comparison of the directional covalent electronic structure between B, a strong cohesion enhancer, and P, a strong embrittler, indicates the strong bonding of the B atom across the boundary plane associated with hybridization of the B 2p electrons with the Fe d band. This directional bonding is not seen in the case of the P atom which does not significantly hybridize with Fe.

The results of the first principles calculations are correlated to the experimental embrittling potency in Figure 5. The difference between grain boundary and free surface segregation energies, calculated by electronic structure calculations, and the experimentally observed shift in the ductile-to-brittle-transition-temperature are plotted for C, B, P and S solutes. The C and B are shown as cohesion enhancers, P and S as embrittlers. The computed energy differences are in excellent agreement with the observed effects on interfacial cohesion. This study is continuing to investigate the embrittling potency of additional solutes as well as ternary solute interactions that may be able to alter the electronic structure of embrittling P and S to reduce their detrimental impact on grain boundary cohesion.

## MATERIALS DESIGN

### Background

In order to illustrate the use of such models in the design of advanced materials we will use the example of case-hardenable secondary hardening gear steels. Design considerations for high performance gears in aerospace, automotive, and other applications drive gear technology to transmit more power in less space and weight. Current high performance gear steels are typically stage I quench and tempered martensites, case hardened through

carburizing to 60 R<sub>C</sub> on the surface with a core hardness of typically 35 R<sub>C</sub>. Gear teeth are cyclically subjected to bending and contact stresses. Failure modes in gears are generally grouped into three categories, tooth breakage, surface pitting, and subsurface spalling. High surface hardness is used to limit the tooth breakage due to bending as well as pitting failures. If the fatigue strength drops below the applied stress

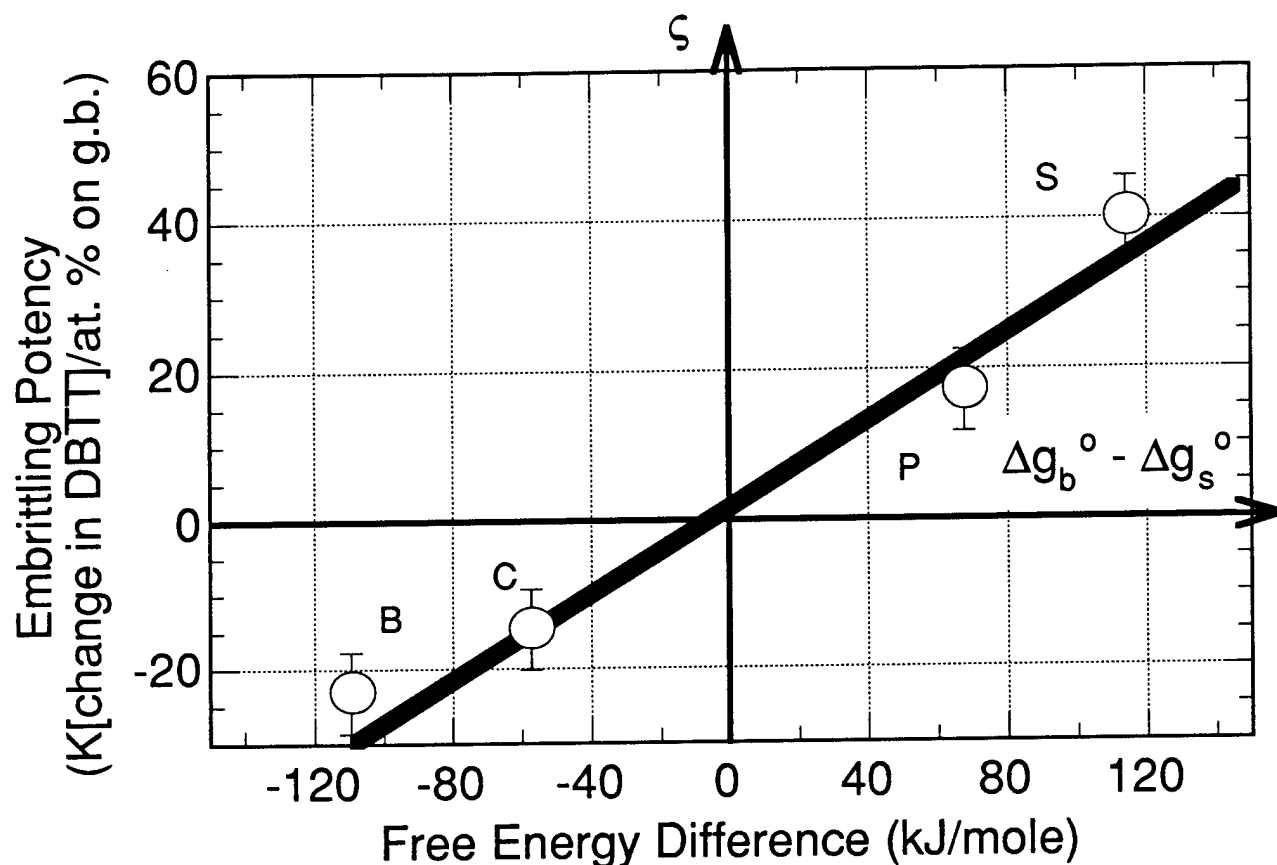


Figure 5 - Correlation between the calculated segregation free energy difference and the experimentally observed embrittling sensitivity (from Ref [17] with new data from [19]).

at any point below the surface, subsurface spalling can result. Typically a 1 mm case depth is required to provide adequate fatigue strength to avoid subsurface spalling.

Stage IV tempered secondary hardening steels offer numerous advantages over conventional gear steels. The efficient strengthening and superior toughness achieved in secondary hardening steels allows greater core and case hardness to be attained reducing the size and weight of gears needed to transmit a given power. The greater temperature resistance of secondary hardening steels allows operation at higher temperatures and longer times before performance degrades. In addition, recent results on commercial secondary hardening alloys indicate casting of these steels may be possible. With these considerations, the Steel Research Group at Northwestern initiated a program to design an advanced secondary hardening case-core gear steel targeted at a 70 R<sub>C</sub> surface hardness with a core hardness of 50 to 55 R<sub>C</sub>. With this increment in material properties, a weight reduction in gear systems of 50% is possible with new gear designs based on these advanced steels. The efforts described in this section represent contributions from many sources, including undergraduate design class and senior projects, one of which received 1st prize in the 1994 TMS Materials Design Competition(20).

## Analysis

The systems analysis of the case-core secondary hardening steel system is the first step in the design process. Figure 6 illustrates the system structure for high power-density gears manufactured by three alternative processing routes, conventional forged ingot processing, near net shape casting and powder processing. Case hardenable secondary hardening gear steels are a subsystem of this flow-block diagram and will be the focus of our discussion. The sequential processing steps dictate the evolution of the case and core microstructures which determine the combination of properties required for the overall performance of the system. Both the case and



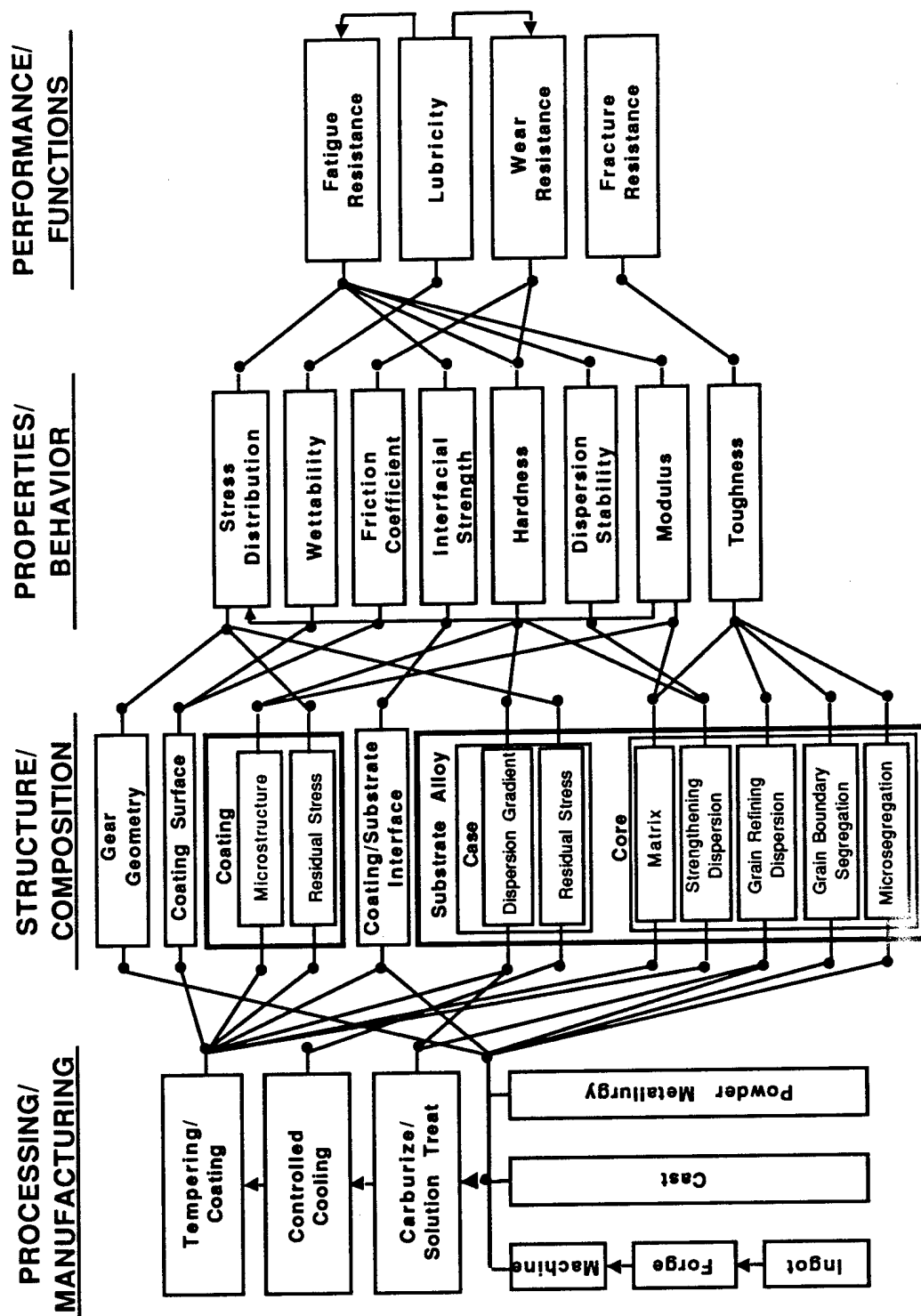


Figure 6 - Flow-block diagram of high power-density gears manufactured from case hardenable secondary hardening gear steel using three alternative processing routes.

core consist microstructures of a lath martensite with high Co for dislocation recovery resistance essential for efficient secondary hardening and Ni for cleavage resistance. Strengthening is provided by the coherent precipitation of fine  $M_2C$  carbides on dislocations. This secondary hardening reaction dissolves the transient cementite and it is essential to bring this reaction to completion in order to eliminate cementite for high toughness. The grain refining dispersion has a double impact on toughness. By limiting grain growth at high temperature during solution treatment, brittle intergranular modes of fracture are avoided. The grain refining particles also play an important role in the ductile microvoid nucleation and coalescence fracture behavior. Thus it is important to preserve adequate volume fraction and size to pin the grain boundaries while choosing the phases with greatest interfacial cohesion. Also important is the control of the grain boundary chemistry to avoid intergranular embrittlement by hydrogen in association with prior segregation of embrittling impurities. During tempering impurities segregate to the grain boundaries and in the case of P and S reduce the interfacial cohesion of the boundary promoting intergranular embrittlement. A number of methods can be used to avoid this problem. Gettering compounds can be utilized to tie up the impurities in stable compounds reducing the segregation to the grain boundary. In order to produce the most stable compounds, however, rapid solidification processing is required. Additional segregants such as B can be deliberately added to enhance intergranular cohesion, and the precipitation rate for the secondary hardening reaction can be increased to limit the time at temperature for harmful grain boundary segregation.

## Design

The first exercise in the design of this steel is to estimate the core and case carbon levels required for the desired hardness. This is done by fitting data for existing secondary hardening Ni - Co steels and extrapolating in a linear fashion to the desired strength. It is estimated that a core carbon content of 0.25 wt% and a case carbon content of 0.55 wt% is needed to provide the desired core and case hardness in this Ni - Co steel.

The next step is to determine the matrix composition of the Fe, Ni, and Co. In order to produce the desired lath martensite morphology, an  $M_s$  temperature of 200 C or above is required. Using a kinetic model for the compositional dependence of the  $M_s$  temperature, the variation with Ni and Co content is determined. This result is illustrated in Figure 7 for the case carbon content using a preliminary composition of the carbide formers equal

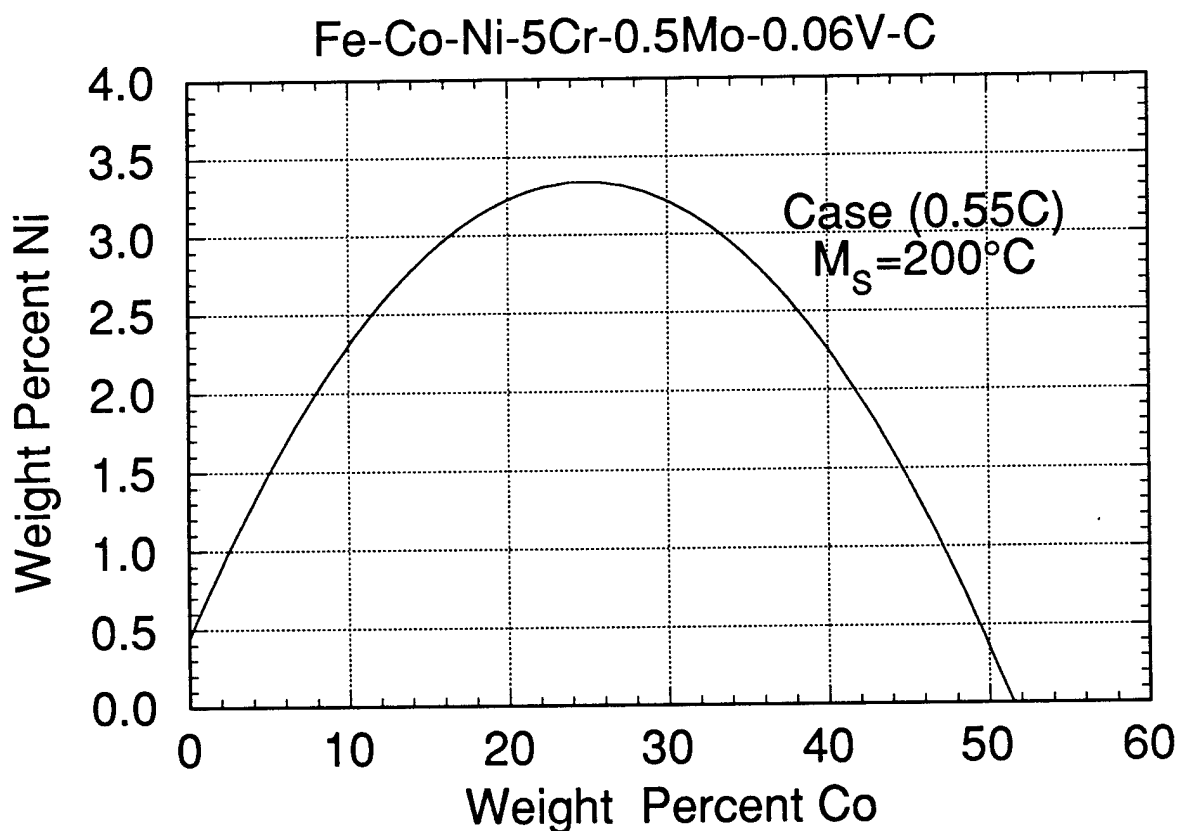


Figure 7 -  $M_s$  temperature calculations for the case composition of the secondary-hardening gear steel(Ref [21]).

to 5 wt% Cr, 0.5 wt% Mo, and 0.06 wt% V. Since the case has a higher carbon content than the core, we can be assured the core will possess a higher  $M_s$  temperature than the case. In Figure 7 the Co and Ni content required to fix the  $M_s$  temperature at 200 C is indicated. Since a high Ni content is desired to avoid cleavage fracture, a composition containing 25 wt% Co is chosen. This allows the highest possible Ni content, approximately 3.5 wt%, to be used. These calculations are later repeated for consistency when the composition of the carbide formers is further refined.

To define the composition of the carbide formers a number of design constraints are applied. The total amount of carbide formers in the alloy must be greater than that required to consume the carbon present in the case. This lower limit insures that, at completion, embrittling cementite is completely converted to  $M_2C$  carbide. In order to reduce grain boundary segregation, the precipitation rate is maximized. This allows the shortest possible tempering time. The coherent precipitation driving force is maximized to provide a small critical particle size for the  $M_2C$  and more efficient strengthening. Finally, the solution temperature is limited to 1000 C. This allows Cr, Mo and V containing carbides such as  $M_{23}C_6$ ,  $M_7C_3$ , MC and  $M_6C$  to be dissolved at reasonable processing temperatures while maintaining very fine scale TiC carbides to act as the grain refining dispersion. Calculations for the precipitation rate constant similar to those outlined in the previous section indicate low Mo compositions are favorable, while driving force calculations have demonstrated the highly beneficial effect of higher V contents. The solubility constraints are presented by the diagram in Figure 8. Here the equilibrium phase fields at 1000 C are given as a function of Cr and V content. The Mo content is determined by the stoichiometry requirements, the matrix composition is taken from the earlier calculations, and the carbon content represents the case composition. The point on the diagram within the single phase FCC field that maximizes the V content and minimizes the Mo content represents the best compromise fulfilling all the design criteria. This composition is 4.8 wt% Cr, 0.03 wt% Mo, and 0.06 wt% V. A recalculation of the matrix composition using the final carbide formers results in an alloy composition of Fe - 25 Co - 3.8 Ni - 4.8 Cr - 0.03 Mo - 0.06 V - 0.55(case)/0.25(core) C (in wt%).

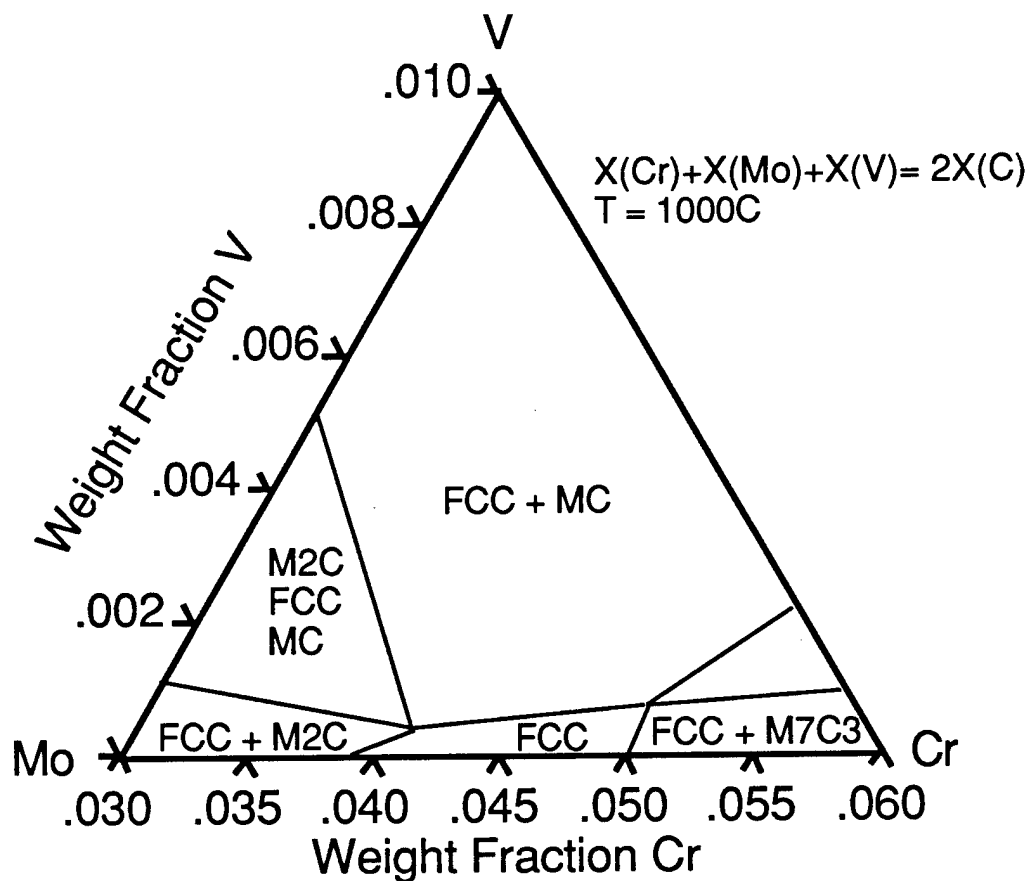


Figure 8 - Phase fields on a pseudo-ternary diagram as a function of Cr, Mo, and V content. The C content is 0.55 wt% and the remaining composition is taken from the matrix composition.

## Prototype Evaluation

A 17 lb. vacuum induction heat of the above composition was prepared by Carpenter Technology Corporation from high purity materials. The ingot was forged at 1150 C in a bar 1.25" square by 38" long. The  $M_s$  temperature of the alloy was determined from dilatometry and found to agree with model predictions. The solution treatment response of the alloy was determined from hardness measurements in the stage I tempered condition. The optimum processing conditions for the core material was determined to be a 1050 C 1 hour solution treatment followed by an oil quench and a liquid nitrogen deep freeze. After optimal solution treatment, a 12 hour temper at 482 C results in the desired overaged hardness of 55  $R_C$  for the core material. The material was then plasma carburized and processed using these parameters. The C potential, temperature and time used in the carburizing treatment were determined from the DICTRA software to provide the target surface carbon content of 0.55 wt% and a 1 mm case depth. Figure 9 represents the hardness profile achieved for the carburized sample. A surface hardness of 67  $R_C$  and a case depth of 1 mm are obtained. Unfortunately, low grain boundary cohesion led to intergranular fracture and limited toughness in this alloy. Based on these results, design work is continuing in order to preserve the excellent strengthening response and improve the toughness in this class of alloy.

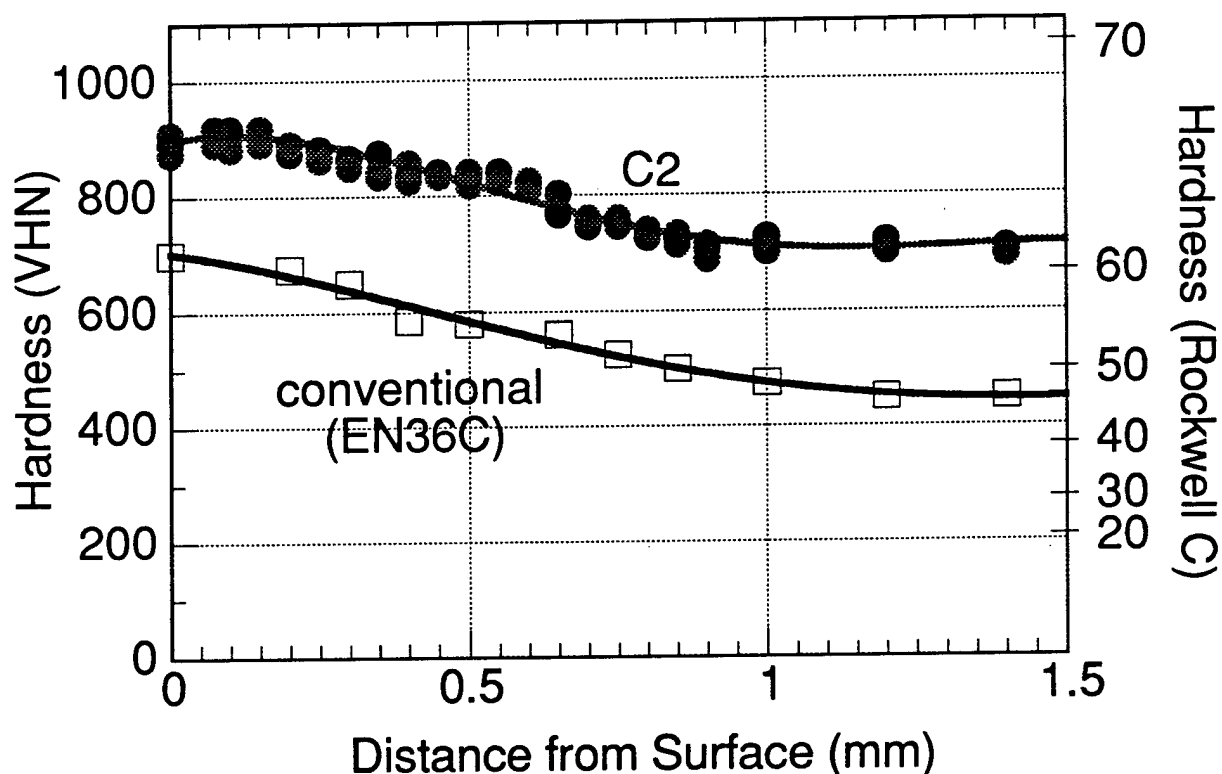


Figure 9 - Carburized hardness profile of prototype secondary hardening gear steel (C2) and conventional gear steel(Ref [22]).

## CONCLUSIONS AND SUMMARY

The above example represents one area of investigation among many at Northwestern University within the SRG and Ferrium Division. A list of materials design efforts, both previous and current, follows:

- Stainless bearing steel for space shuttle main engine turbopumps (patented).
- Aircraft armor steels.
- Oxide superconductors.
- Ferritic stainless superalloys.
- Low-cost secondary hardening gear steels.
- Ultrahigh-strength austenitic TRIP steels.
- Biomedical Co based corrosion resistant alloys.
- Alloys for high pressure fuel injectors.

- Dental concrete/Polymer composites.
- Polymer based case hardened gears.
- Mg based semi-solid casting alloys.
- Self-Healing biomimetic superalloy composites.

The key to successfully addressing these design challenges rests with the development of quantitative models as design tools and using them in a systems-based approach to the design of new materials. The above examples illustrate both the care that must be exercised in the development of quantitative useful modelling, and the deliberate manner in which they need to be used. Advances in computational modelling and computer power insure that computational metallurgy will play an increasing role in defining the discipline of materials science and engineering.

## ACKNOWLEDGEMENTS

The SRG program is supported NASA, ONR, ARO, DOE, AFOSR, and NSF, with additional industrial fellowship support. The model alloys employed in the secondary hardening modelling were provided by the NKK Corporation of Hiroshima, Japan and were evaluated by Shigeru Endo. Development of the prototype gear steel was accomplished with funding from the Ford Motor Company of Dearborn Michigan.

## REFERENCES

1. G.M. Jenkins, The Systems Approach, Open University Press, 1972.
2. C.S. Smith, A Search for Structure, MIT Press, Cambridge, MA, 1981.
3. G.B. Olson, "Materials Design: An Undergraduate Course" Morris E. Fine Symposium, P. K. Liaw, J. R. Weertman, H. L. Marcus and J. S. Santner, Eds., The Minerals, Metals & Materials Society, 1991.
4. B. Sundman, B. Jansson and J.O. Andersson, "The Thermo-Calc Databank System", CALPHAD, Vol. 9, 1985, 153-190.
5. G.M. Carinci, G.B. Olson, J.A. Liddle, L. Chang and G.D.W. Smith, "AP/FIM Study of Multicomponent  $M_2C$  Precipitation" Innovations in Ultrahigh-Strength Steel Technology (34th Sagamore Army Materials Research Conference), G. B. Olson, M. Azrin and E. S. Wright, Eds., U. S. Government Printing Office, Washinton DC, Lake George, NY, 1987, 179-208.
6. G.B. Olson, T.J. Kinkus and J.S. Montgomery, "APFIM Study of Multicomponent  $M_2C$  Carbide Precipitation in AF1410 Steel", Surface Science, Vol. 246, 1991, 238-245.
7. J.S. Montgomery and G.B. Olson, " $M_2C$  Carbide Precipitation in AF1410" 1992 Spiech Symposium, 1992, 177-214.
8. A.J. Allen, D. Gavillet and J.R. Weerman, "SANS and TEM studies of Isothermal  $M_2C$  Carbide Precipitation in Ultrahigh Strength AF1410 Steel", Acta Metall. Mater., Vol. 41, 1993, 1869-1884.
9. P. Jemian, unpublished research, Northwestern University, 1991.
10. J.S. Langer and A.J. Schwartz, "Kinetics of Nucleation in Near-Critical Fluids", Phys. Rev. A, Vol. 21, 1980, 948-958.
11. K.C. King, G.B. Olson and T. Mura, Elastic Energy of Coherent Precipitation at Dislocations in an Anisotropic Matrix, The Society for Industrial and Applied Mathematics, Philadelphia, PA, 1991, .
12. K.C. King, P.W. Voochees, G.B. Olson and T. Mura, "Solute Distribution Around a Coherent Precipitate in a Multicomponent Alloy", Met. Trans. A, Vol. 22, 1991, 2199-2210.
13. I.M. Lifshitz and V.V. Slyozov, "The Kinetics of Precipitation from Supersaturated Solid Solutions", J. Phys. Chem. Solids, Vol. 19, 1961, 35-50.

14. C. Wagner, "Theorie der Alterung von Niederschlagen durch Umlosen", Z. Elektrochem, Vol. 65, 1961, 581-591.
15. C.J. Kuehmann and P.W. Voorhees, Metall. Trans. A, In Press.
16. A. Umantsev and G.B. Olson, "Ostwald Ripening in Multicomponent Alloys", Scripta Met., Vol. 29, 1993, 1135-1140.
17. J.R. Rice and J.-S. Wang, "Embrittlement of Interfaces by Solute Segregation", Mater. Sci. Eng., Vol. A107, 1989, 23-40.
18. P.M. Anderson, J.S. Wang and J.R. Rice, "Thermodynamic and Mechanical Models of Interfacial Embrittlement" Innovations in Ultrahigh-Strength Steel Technology (34th Sagamore Army Materials Research Conference), G. B. Olson, M. Azrin and E. S. Wright, Eds., U. S. Government Printing Office, Washinton DC, Lake George, NY, 1987, 619-649.
19. R. Wu, A.J. Freeman and G.B. Olson, "First Principles Determination of the Effects of Phosphorus and Boron on Iron Grain-Boundary Cohesion", Science, July 15, 1994, 376-380.
20. D.J. Cook and G.A. Lewis, "High Performance Secondary-Hardening Gear Steel Design and Evaluation: The C2 Prototype", 1994, Northwestern University.
21. C. Campbell, Northwestern University, unpublished research.
22. J. Wise, Northwestern University, unpublished research.